Research Article

Journal of Physical Organic Chemistry

Received: 21 March 2008, Revised: 24 September 2008, Accepted: 20 October 2008, Published online in Wiley InterScience: 15 December 2008

(www.interscience.wiley.com) DOI 10.1002/poc.1492

The mechanism of alkaline hydrolysis of amides: a comparative computational and experimental study of the hydrolysis of *N*-methylacetamide, *N*-methylbenzamide, and acetanilide

Diana Cheshmedzhieva[a], Sonia Ilieva[a], Boriana Hadjieva[a] and Boris Galabov[a]*

Theoretical computations and experimental kinetic measurements were applied in studying the mechanistic pathways for the alkaline hydrolysis of three secondary amides: *N*-methylbenzamide, *N*-methylacetamide, and acetanilide. Electronic structure methods at the HF/6-31+G(d,p) and B3LYP/6-31+G(d,p) levels of theory are employed. The energies of the stationary points along the reaction coordinate were further refined via single point computations at the MP2/6-31+G(d,p) and MP2/6-311++G(2d,2p) levels of theory. The role of water in the reaction mechanisms is examined. The theoretical results show that in the cases of *N*-methylbenzamide and *N*-methylacetamide the process is catalyzed by an ancillary water molecule. The influence of water is further assessed by predicting its role as bulk solvent. The alkaline hydrolysis process in aqueous solution is characterized by two distinct free energy barriers: the formation of a tetrahedral adduct and its breaking to products. The results show that the rate-determining stage of the process is associated with the second transition state. The entropy terms evaluated from theoretical computations referring to gas-phase processes are significantly overestimated. The activation barriers for the alkaline hydrolysis of *N*-methylbenzamide and acetanilide were experimentally determined. Quite satisfactory agreement between experimental values and computed activation enthalpies was obtained. Copyright © 2008 John Wiley & Sons, Ltd.

Supporting information may be found in the online version of this article.

Keywords: base hydrolysis; amide; reaction mechanism; *ab initio* computations; density functional theory computations

INTRODUCTION

The hydrolysis of secondary amides is an extensively studied process because it is regarded as a model for the cleavage of the peptide bond.[1] The reactions in alkaline and neutral media correspond most closely to the conditions usually found in the living systems. The reaction has been in the focus of numerous experimental kinetic[2–43] and theoretical studies.[44–84] The following general scheme (Scheme 1) for the alkaline hydrolysis of amides is suggested:[27]

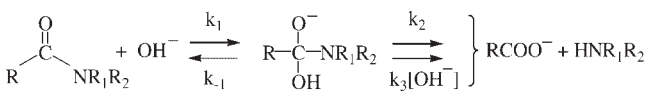

Scheme 1. General scheme for the alkaline hydrolysis of amides.

In experimental conditions the amide hydrolysis takes usually place in water medium. It is, therefore, important to analyze the specific influences of water on the process as a medium but also its possible interaction with the reactants and its role on the mechanistic pathway. A number of studies discussed the promoting role of water molecules on the hydrolysis of amides.[48,51,54,55,59,62,63,69,71,73,74,76,80–84] Bakowies and Kollman[59] carried out a theoretical analysis of the base-catalyzed hydrolysis of formamide in water. These authors applied a combination of high-level *ab initio* computations as well as Monte Carlo simulations to model the mechanism of the process in the gas phase and in aqueous solution. Three principal stages of the base-catalyzed hydrolysis were considered: the formation of a tetrahedral intermediate, its conformational isomerization and, finally, the breakdown to products. The authors underlined the substantial differences of the reaction path in the gas phase and in water solution. The solvent causes a significant barrier toward the formation of the adduct, while facilitating its

* *Correspondence to: Prof. B. Galabov, Department of Chemistry, University of Sofia, 1 James Bourchier Ave., 1164 Sofia, Bulgaria. E-mail: galabov@chem.uni-sofia.bg*

a *D. Cheshmedzhieva, S. Ilieva, B. Hadjieva, B. Galabov Department of Chemistry, University of Sofia, 1 James Bourchier Ave., 1164 Sofia, Bulgaria*

isomerization. It is shown also that an ancillary water molecule, hydrogen bonded to the tetrahedral intermediate, assists its breakdown to products. Karplus and co-workers[75] also examined the effect of an ancillary water molecule on the second step of the reaction (TS2) and found that the inclusion of an explicit molecule significantly decreases the TS2 barrier. The predicted effect in these studies is a substantial stabilization of the transition states by the water molecule. Pitarch *et al.*[71] studied theoretically the participation of an ancillary water molecule in the mechanism of neutral and alkaline hydrolysis of the beta-lactam *N*-methylazetidinone. Correlated *ab initio* computations of these authors showed that the additional water molecule leads to a reduced free-energy barrier for the process. In a recent computational study Mujika *et al.*[76] applied density functional theory in studying a water-assisted hydrolysis of an amide twisted along the C—N bond. It was shown that an ancillary water molecule assists the proton transfer processes along the reaction path. Brown and co-workers[25] applied NMR spectroscopy to study the base-catalyzed hydrolysis of formamide. These authors considered both nucleophilic and general base catalyzed mechanisms. They found that both type of mechanisms can be accommodated within the results from a proton inventory analysis. The results indicated that a nucleophilic mechanism, that is, direct attack of the OH^- at the C═O reaction center is preferred.

Xiong and Zhan[69] conducted recently a theoretical study on the base-catalyzed hydrolysis of formamide, *N*-methylacetamide, dimethylformamide, and dimethylacetamide. The authors examined in detail the solvent effect on the formation of the tetrahedral intermediate, which was considered as the rate-determining step. This study underlined the role of the solvating water molecules on the energy profiles of the hydrolysis process. Conflicting reports regarding the rate-limiting stage of alkaline hydrolysis of secondary amide are found in the literature.[2–14,18,19,25,27,33,50,51,62–65,69]

In the present work we apply first principles electronic structure computations to study the mechanistic pathways for the alkaline hydrolysis of three secondary amides: *N*-methylbenzamide, *N*-methylacetamide, and acetanilide. The bulk solvent effect of the water solvent was assessed. The catalytic role of an explicit ancillary water molecule on the process was also examined. It was expected that the substitution by aromatic rings at both side of the amide grouping would provide valuable information regarding the influence of conjugative effects on the base-catalyzed amide hydrolysis. It was also of interest to follow the relative energy barriers for the two principal stages of the process and analyze the effect of structural variations. In earlier studies from this laboratory[77,78] on a series of acetanilide derivatives substituted in the aromatic ring it was shown that a stepwise mechanism is the most favored path of the process.

THEORETICAL METHODS AND KINETIC EXPERIMENTS

Details of computatinal methods

The theoretical computations were performed by employing the Hartree–Fock method with 6-31+G(d) basis set[85] and density functional theory (DFT) employing the B3LYP hybrid functional[86,87] and 6-31+G(d,p) basis set. The basis sets include diffuse functions for proper description of anionic transition states.[88] Stable structures and transition states were fully optimized at the HF and DFT level of theory by traditional transition state optimization using the Berny algorithm.[89] All critical points were further characterized by analytic computations of harmonic vibrational frequencies at the same level/basis sets. All transition structures were checked by intrinsic reaction coordinate (IRC) calculations.[90,91] These computations were carried out with the Gaussian 98 program package.[92]

Solvent effects were examined using the Integral Equation Formulation of the Polarizable Continuum Model (IEFPCM)[93,94] incorporated in Gaussian 03.[95] In this approach, the solvent is represented by a homogenous continuum medium, which is polarized by the solute placed in a cavity. The cavity was specified using the UFF atomic radii.[96] The solute–solvent interactions are described in terms of a solvent reaction field, which can be partitioned into dispersion, repulsive and electrostatic forces between solute and solvent molecules.[93] Single point IEFPCM B3LYP/6-31+G(d,p) computations were performed for estimating the influence of water on the energies of all structures along the reaction path. The theoretically estimated energies of the stationary points along the reaction paths were further refined by single point MP2[97–101] computations employing the 6-31+G(d,p) and 6-311++G(2d,2p) basis sets[101,102] combined with the IEFPCM method for assessing the effect of water.

Kinetic experiments

The kinetics of the alkaline hydrolysis *N*-methylbenzamide (**MBA**) and acetanilide (**AA**) were studied using UV spectroscopy. The change in absorbance due to the reactant amides and the products was followed on Unicam UV500 spectrometer. The hydroxide ion concentration was 0.9 M and the ionic strength was maintained constant at 0.9 M (NaCl). The initial concentrations of amides were: 1×10^{-4} M for **AA** and 1.5×10^{-3} M for **MBA**. The hydroxide concentration was in large excess and the reactions exhibited pseudo-first-order kinetics. Kinetic data were generated to estimate the rate constants, k_{obs}, by plotting $\ln(C/C_0)$ *versus* time. The slope of the line yielded k_{obs}. Kinetic measurements were carried out at four different temperatures: 25, 45, 65, and 85 °C in the case of **AA** and 65, 75, 85, and 95 °C for **MBA**. Temperatures were kept constant by a thermostat to within ±0.1 °C. The reactions were followed to over 80% transformation of the initial amides. In determining the concentrations we used the Vierordt[103] equations for analysis of two component mixtures because of overlap of the absorption bands of reactants and products. The analytical wavelengths used were 238 and 281 nm in the case of acetanilide, and 260 and 278 nm – for *N*-methylbenzamide. In every case the k_{obs} is the average of three independent measurements. From the collected kinetic data free energy barrier heights, enthalpies, and entropies of activation were derived.

RESULTS AND DISCUSSION

As already emphasized the focus of the present study is the comparative analysis of the factors that influence the reaction path for the alkaline hydrolysis of three representative secondary amides: *N*-methylacetamide (**MAA**), *N*-methylbenzamide, and acetanilide. No theoretical results on the mechanism of hydrolysis of **MBA** have been reported so far. Thus we carried out a detailed

study of this reaction in gas phase and in water solution. The alkaline hydrolysis reactions in the cases of **MAA** and **AA** were studied previously using electronic structure methods.[50,51,62–65,69,77,84,104] However, different levels of theory were applied and, therefore, the comparisons of the energy profiles of the processes was not possible. To overcome this problem we performed theoretical computations to optimize all critical structures along the reaction paths for **MAA** and **AA** at the same levels of theory as used in the case of **MBA.** It was hoped that the comparative approach would allow to shed light on specific features of the hydrolysis of secondary amides that cannot be fully appreciated from the usual studies on a single derivative. As mentioned, we analyzed the energy profiles of the processes in the gas phase, the effect of ancillary water on the energetics as well as the influence of the bulk water solvent.

As is well known, a critical point in all computational studies is the correspondence between the theoretical results obtained and the respective available experimental data. As it turned out, however, no kinetic data on the energetics of the reactions of **MBA** and **AA** were available in the literature. The activation energy of the process was only reported for **MAA**.[105] To fill this gap we carried out variable temperature kinetic studies for the alkaline hydrolysis of **MBA** and **AA**. These data were then used to assess the overall reliability of the theoretical predictions obtained.

Alkaline hydrolysis in the gas phase

Mechanism of the alkaline hydrolysis of N-methylbenzamide in the gas phase

Since the amide hydrolysis takes usually place in water media, the study of the mechanism of the process in the gas phase appears less important. However, it is of interest to follow the changing energy profiles of the reactions of the three amides studied in going form gas phase to water-assisted and in bulk water solvent. It should be pointed out that in presence of water the process differs quite considerably from the gas phase reaction. In water media the hydroxide ion and H_2O should not be considered as separate reactants. As will be discussed later, an acceptable model system reflecting the quick interaction between these two reactants is the respective hydrogen-bonded complex. In effect, in presence of water it is correct to consider this complex as the real reactant species, rather than the individual components. This complex satisfies the high demand for solvation of the hydroxide ion.

The hydrolysis of *N*-methylbenzamide begins with an attack of the nucleophilic hydroxide ion at the electrophilic carbon atom of the carbonyl group. The calculated optimized structures (B3LYP/6-31+G(d,p)) for the stationary points along the reaction pathway of the alkaline hydrolysis of **MBA** are shown in Fig. 1. A tetrahedral intermediate between **MBA** and the hydroxide ion is formed as a first stage of the process. This is the nucleophilic addition step and it goes through a transition state **TS1–MBA** (Fig. 1). The transition state structure reflects the creation of a C—O bond. The changes of selected bond lengths along the reaction path are presented in Fig. 1. The normal mode vector of the imaginary frequency for **TS1–MBA** transition state depicts the motion of the oxygen atom from the hydroxide ion toward the carbonyl carbon. The $C\cdots OH^-$ distance in the transition structure **TS1–MBA** is 2.110 Å and the length of the carbonyl bond r_{CO} is 1.244 Å. This is an early reactant-like transition state. The r_{CO} distance shows that the carbonyl double bond is still present.

The relative energies of all the structures along the reaction pathway of the alkaline hydrolysis of **MBA** with respect to

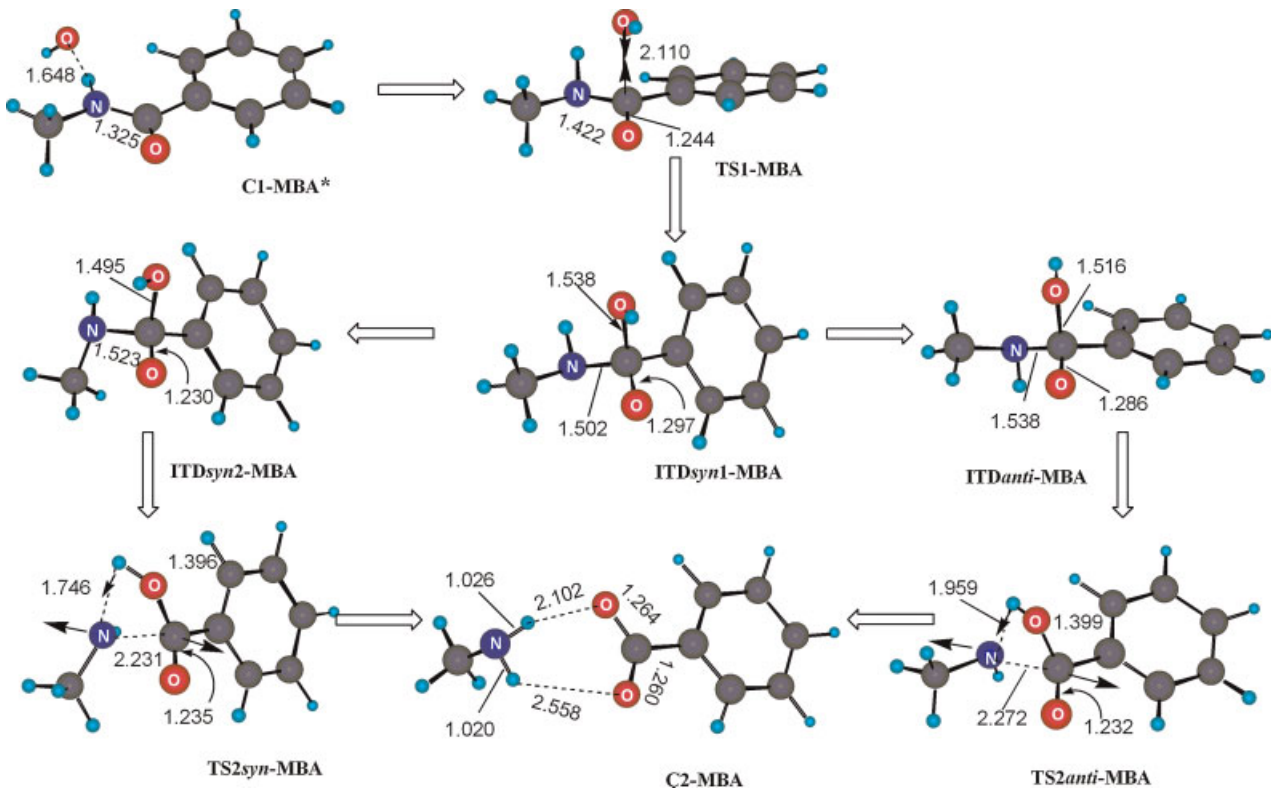

Figure 1. Optimized structures along the reaction pathway for the base hydrolysis of *N*-methylbenzamide (MBA) from B3LYP/6-31+G(d,p) computations

Table 1. Relative to reactants energies, ΔE (in kcal/mol), and free energies, ΔG (at 1 atm, 298.15 K, in kcal/mol) for intermediates, transition states and products along the mechanistic pathway of the alkaline hydrolysis of *N*-methylbenzamide in the gas phase from HF/6-31+G(d) and B3LYP/6-31+G(d,p) computations

	HF/6-31+G(d)		B3LYP/6-31+G(d,p)	
Structures	ΔE[a]	ΔG	ΔE[a]	ΔG
R[b]	0.00	0.00	0.00	0.00
C1-MBA	−35.74	−27.43	−38.18[c]	−28.89[c]
TS1-MBA	−9.45	−0.70	−16.48	−7.29
ITD*syn1*-MBA	−19.99	−10.67	−20.78	−11.49
ITD*syn2*-MBA	−18.34	−8.85	−19.55	−10.00
TS2*syn*-MBA	2.12	10.61	−8.43	0.41
ITD*anti*-MBA	−14.20	−4.71	−16.32	−6.66
TS2*anti*-MBA	6.78	15.40	−2.40	6.35
P	−53.03	−55.55	−46.68	−48.94

[a] Corrected for zero-point vibrational energy.
[b] Reactants are the amide and the OH^-.
[c] The thermal corrections are taken from ***ITDsyn1-MBA*** structure.

reactants are given in Table 1 and schematically presented in Fig. 2. The estimated relative to reactants free energy (ΔG) of the first transition state **TS1–MBA** for the hydroxide attack is −7.29 kcal/mol. IRC computations at the Hartree–Fock level in backward direction showed that **TS1–MBA** converts into a pre-reactive complex between the reactants denoted as **C1–MBA**. Analogous DFT computations, however, did not converge to such structure. Similar ion-dipole complexes between the reactants in amide hydrolysis have been optimized previously in the cases of *N*,*N*-dimethylacetamide[68] and acetanilide[77] at the HF/6-31+G(d) level of theory.

Since in the gas phase **TS1–MBA** is lower in energy than the reactants, the process could be regarded as barrierless. An intrinsic activation barrier can, however, be defined with respect the prereactive complex **C1–MBA**. In a study on the hydrolysis of *N*-methylazetidinone[70] the authors state that a tetrahedral intermediate is directly formed and consider unlikely that such an ion-dipole complex can exist in the gas-phase. As we will see in the next part, however, the formation of such a complex in presence of explicit water molecule is predicted by both HF and DFT computations for the hydrolyses of **MAA** and **MBA**.

The IRC computations in forward direction from **TS1** to **MBA** lead to a stable tetrahedral intermediate **ITD*syn1*–MBA**, in which a C—OH bond is created (1.538 Å, Fig. 1) and the carbonyl carbon atom becomes a tetrahedral center. Different conformers of the tetrahedral intermediate can be involved in the reaction. The rotameric forms denoted as **ITD*syn1***, **ITD*syn2***, and **ITD*anti*** as obtained from IRC computations from **TS1**, **TS2*syn***, and **TS2*anti*** are illustrated in Scheme 2. These structures are found for all three secondary amides studied. The syn and anti forms are associated with the orientation of the hydroxyl hydrogen with respect to the carbonyl oxygen in the CO^-(OH) grouping. O'Brien and Pranata[67] explored the conformational potential energy surface of the tetrahedral intermediate of *N*-methylformamide. These authors considered two most important rotameric forms of the tetrahedral intermediates among many possible structures, denominated as syn and anti conformers. These forms are illustrated in Scheme 2. O'Brien and Pranata have shown that these two forms are in fact related to the respective **TS2** structures.

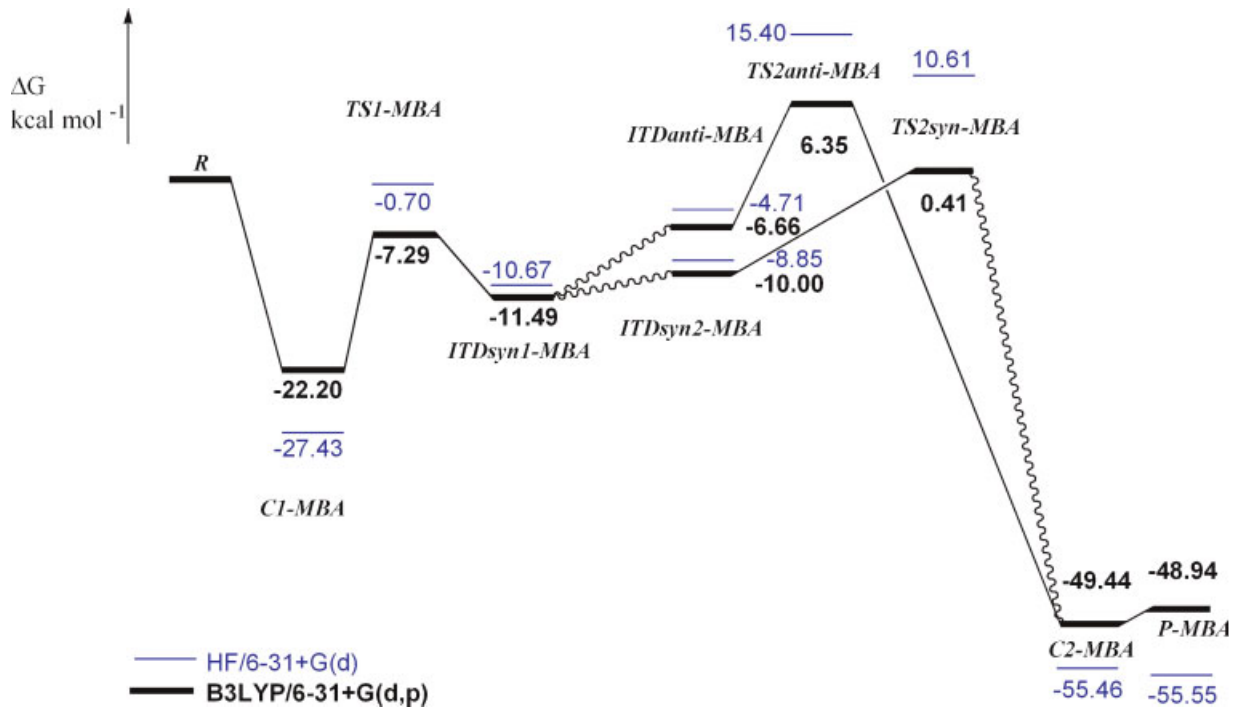

Figure 2. Energy diagram of the gas phase mechanism for the unassisted alkaline hydrolysis of *N*-methylbenzamide (MBA)

Journal of Physical Organic Chemistry

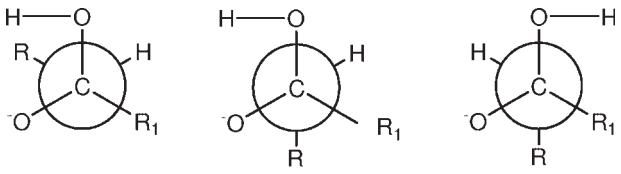

Scheme 2. Newman projections of conformers of the tetrahedral intermediates as obtained from IRC computations

The conformers with *syn* CO^-(OH) grouping are more stable because of favorable interaction between the C—O^- and O—H bond dipoles.[67] On the other hand, the *anti* —CO^-(OH) conformation favors the next step of the reaction in the case of **AA**[77] because of plausible orientation of the proton from the OH group to the nitrogen lone pair. As underlined by Bakowies and Kollman,[59] a transition to a more favorable for the second transition state conformation is an important step in the hydrolysis mechanism. The **ITD*syn1*** and **ITD*syn2*** and **ITD*anti*** conformations in the case of **MBA** are shown in Fig. 1.

The next stage of the process involves the cleavage of the amide C—N bond and simultaneous restoration of the carbonyl double bond. It is often named as elimination step or breaking of the tetrahedral intermediate. The reaction can proceed further through both *anti* (**TS2*anti*-MBA**) and *syn* (**TS2*syn*–MBA**) pathways. The transition vectors for the two **TS2** structures correspond basically to the cleavage of the amide C—N bond yielding recovery of the C=O double bond. Forward IRC calculations from the second transition state **TS2** result in a stable complex between the acetate anion and the amine that can be regarded as post-reactive complex **C2** (Fig. 1) for both *syn* and *anti* conformations. The overall energetics of the alkaline hydrolysis of **MBA** in gas phase is represented in Fig. 2.

Alkaline hydrolysis of N-methylacetamide and acetanilide in the gas phase

As mentioned, the base hydrolyses of *N*-methylacetamide and acetanilide have been studied earlier.[50,62–65,69,77,84,104] Though there are numerous theoretical studies on *N*-methylacetamide we calculated the energies of the stationary points along the reaction paths using the same method/basis sets as those employed in the case of **MBA**. In the case of acetanilide the HF results were directly taken from Ref.[77] The respective B3LYP/6-31+G(d,p) values for **AA** were, however, recalculated for consistency of data for the three amides. In Tables 2 and 3 the energies of the stationary point structures along the reaction paths of **MAA** and **AA** are presented. The symbols used for the different species along the process pathways are analogous to those used in the case of *N*-methylbenzamide. Again for these molecules, in absence of explicit water molecule, a pre-reactive complex could not be obtained from IRC computations using the B3LYP/6-31+G(d,p) level of theory. In general, the mechanistic pathways for the alkaline hydrolysis of **MAA** and **AA**, encompass similar stationary point structures as in the case of **MBA**. However, the energies of these structures may differ quite considerably from molecule to molecule. These differences determine also variations in the rate-determining stage of the process as well. It is seen (Fig. 3) that the reaction pathways for the hydrolysis of **MBA** and **MAA** are quite similar. The energy of **TS2** for acetanilide is, however, much lower then in the other two molecules. For the gas phase process in **AA** the formation of the tetrahedral adduct is the rate-determining step, in contrast to **MBA** and **MAA**. The Gibbs free energies of the gas phase processes for the three molecules considered show that the rate-determining step is associated with the second transition states (Tables 1 and 2). In the case of acetanilide **AA** (Table 3) ΔG for **TS1–AA** (−10.86 kcal/mol) is predicted to have higher value than **TS2anti-AA**. The difference is, however, just 1.1 kcal/mol.

Table 2. Relative to reactants energies, ΔE (in kcal/mol), and free energies, ΔG (at 1 atm, 298.15 K, in kcal/mol) for intermediates, transition states and products along the mechanistic pathway for the alkaline hydrolysis of *N*-methylacetamide in the gas phase from HF/6-31+G(d) and B3LYP/6-31+G(d,p) computations

	HF/6-31+G(d)		B3LYP/6-31+G(d,p)	
Structures	ΔE[a]	ΔG	ΔE[a]	ΔG
R[b]	0.00	0.00	0.00	0.00
C1-MAA	−31.71	−23.19	—	—
TS1-MAA	−8.17	2.26	−13.52	−4.59
ITD*syn*-MAA	−15.44	−4.74	−16.69	−7.32
ITD*anti*-MAA	−9.17	1.49	−11.17	−1.78
TS2*anti*-MAA	6.18	16.18	−2.16	6.42
P	−44.65	−45.66	−38.53	−41.80

[a] Corrected for zero-point vibrational energy.
[b] Reactants are the amide and the OH^-.

Water-assisted alkaline hydrolysis of N-methylbenzamide, N-methylacetamide, and acetanilide

Table 3. Relative to reactants energies, ΔE (in kcal/mol), and free energies, ΔG (at 1 atm, 298.15 K, in kcal/mol) for intermediates, transition states and products along the mechanistic pathway for the alkaline hydrolysis of acetanilide in the gas phase from HF/6-31+G(d) and B3LYP/6-31+G(d,p) computations

	HF/6-31+G(d)[a]		B3LYP/6-31+G(d,p)	
Structures	ΔE[b]	ΔG	ΔE[b]	ΔG
R[c]	0.00	0.00	0.00	0.00
C1-AA	−40.12	−31.26	—	—
TS1-AA	−15.35	−4.98	−20.31	−10.86
ITD*syn*1-AA	−29.48	−17.01	−35.42	−18.91
ITD*anti*-AA	−21.90	−9.51	−22.24	−12.49
TS2*anti*-AA	−16.49	−5.68	−21.36	−11.98
P	−51.37	−53.22	−43.93	−47.34

[a] From Ref. [77]
[b] Corrected for zero-point vibrational energy.
[c] Reactants are the amide and the OH^-.

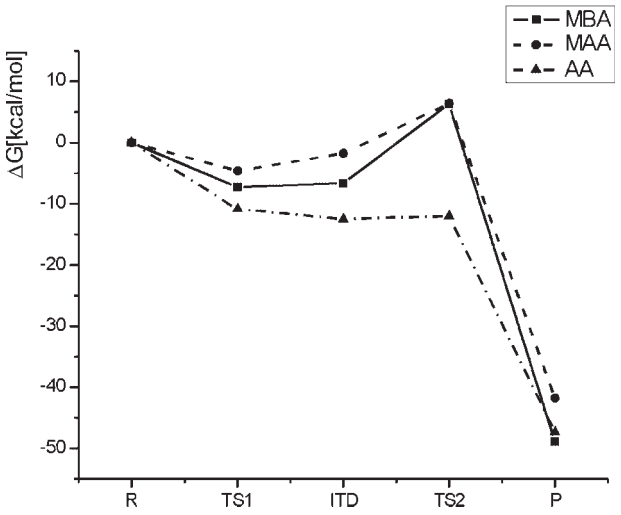

Figure 3. Energy profiles for the hydrolysis of MBA, MAA, and AA in the gas phase from B3LYP/6-31+G(d,p) computations

The natural reaction medium for the hydrolysis process is water. It is, therefore, essential to analyze the role of water on the mechanism and energetics of the processes as well as its influence as a bulk solvent. The participation of an ancillary water molecule in the reaction pathway was first considered. As already discussed, in presence of water the OH^- reactant is transformed into ion-molecule complex. The free energy gain from this process is estimated at 23.69 kcal/mol from B3LYP/6-31+G(d,p) computations. The role of explicit water molecules on the process has been studied for neutral,[71,82] alkaline,[59,71,75] and acid-promoted amide hydrolysis.[54,55,64,82]

In the present study the influence of an ancillary water molecule on the mechanism of alkaline hydrolysis of *N*-methylbenzamide (**MBA**), *N*-methylacetamide (**MAA**), and acetanilide (**AA**) is considered. Most critical structures – reactants, products, intermediates, and transition states – along the hydrolysis pathways of **MBA**, **MAA**, and **AA** in the presence of an ancillary water molecule were optimized at HF/6-31+G(d) and B3LYP/6-31+G(d,p) levels of theory. The theoretically computed energies of the stationary points are summarized in Tables 4–6. Interestingly, with the addition of water molecule the structure of the prereactive complex was successfully optimized at both Hartree–Fock and DFT computations for the reactions of **MBA** and **MAA**. The **C1** complex and the **TS2** structure for hydrolysis of acetanilide could only be optimized at HF/6-31+G(d) level of theory. The respective **C1** and **TS2** energies were obtained from single point B3LYP/6-31+G(d,p) computations. As in the case of initial hydroxide ion, the auxiliary water molecule stabilizes the pre-reactive complex. This stabilizing effect can be further enhanced if more explicit water molecules are considered.[69,79]

The presence of an auxiliary water molecule does not alter substantially the structure of the first transition state, though **TS1** for the three amides are distinctly more stable compared to the transition states in absence of water. The **TS1** structures corresponding to attack of the hydroxide ion at the carbonyl carbon atom and leading to the formation of tetrahedral intermediates are schematically represented in Fig. 4 for the water-assisted hydrolysis of **MBA** (A), **MAA** (B), and **AA** (C). The distance between the oxygen atom from the attacking hydroxide anion and the carbonyl carbon atom in **TS1** is 1.798 Å in the case of **MBA**, 1.803 Å for **MAA**, and 2.094 Å for **AA** (Fig. 4). These distances are markedly shorter compared to those computed for the **TS1** structures in the case of non-assisted gas phase process (2.110 Å for **MBA**, 2.168 Å for **MAA**, and 2.214 Å for **AA** (Fig. 1)). As can be seen from the structures and corresponding distances presented in Fig. 4, the assisting water

Table 4. Relative to reactants energies, ΔE (in kcal/mol), and free energies, ΔG (at 1 atm, 298.15 K, in kcal/mol) for intermediates, transition states and products along the mechanistic pathway for the alkaline hydrolysis *N*-methylbenzamide with participation of an explicit water molecule from HF/6-31+G(d) and B3LYP/6-31+G(d,p) computations

	HF/6-31+G(d)		B3LYP/6-31+G(d,p)	
Structures	ΔE[a]	ΔG	ΔE[a]	ΔG
R[b]	0.00	0.00	0.00	0.00
C1–W-MBA	−29.70	−20.55	−31.22	−21.45
TS1–W-MBA	1.19	13.09	−0.45	11.61
ITD*syn1*–W-MBA[c]	−11.29	−0.60	−6.15	5.38
ITD*syn2*–W-MBA[c]	−10.98	0.76	−6.11	5.95
TS2*syn*–W-MBA[c]	12.09	25.32	2.00	14.47
ITD*anti*–W-MBA[c]	−0.39	11.07	1.99	13.51
TS2*anti*–W-MBA[c]	11.95	24.71	3.70	16.57
P	−30.40	−38.90	−16.82	−25.26

[a] Corrected for zero-point vibrational energy.
[b] Reactants are the amide and the $[OH...H_2O]^-$ complex.
[c] The different conformers of the intermediates and TS2 are illustrated in Fig. 1 in the case of *N*-methylbenzamide.

Table 5. Relative to reactants energies, ΔE (in kcal/mol), and free energies, ΔG (at 1 atm, 298.15 K, in kcal/mol) for intermediates, transition states and products along the mechanistic pathway for the alkaline hydrolysis *N*-methylacetamide with participation of an explicit water molecule from HF/6-31+G(d) and B3LYP/6-31+G(d,p) computations

	HF/6-31+G(d)		B3LYP/6-31+G(d,p)	
Structure	ΔE[a]	ΔG	ΔE[a]	ΔG
R[b]	0.00	0.00	0.00	0.00
C1–W-MAA	−26.74	−17.28	−28.05	−18.37
TS1–W-MAA	1.85	15.21	1.34	14.89
ITD*syn1*–W-MAA[c]	−3.55	10.80	−3.29	9.30
ITD*syn2*–W-MAA[c]	−6.55	6.35	−2.23	10.59
TS2*syn*–W-MAA[c]	16.30	30.40	7.23	20.73
ITD*anti*–W-MAA[c]	3.31	15.84	4.95	17.47
TS2*anti*–W-MAA[c]	14.45	28.34	7.75	21.37
P	−22.02	−29.03	−8.78	−17.00

[a] Corrected for zero-point vibrational energy.
[b] Reactants are the amide and the $[OH...H_2O]^-$ complex.
[c] The different conformers of the intermediates and TS2 are illustrated in Fig. 1 in the case of **MBA**.

Table 6. Relative to reactants energies, ΔE (in kcal/mol), and free energies, ΔG (at 1 atm, 298.15 K, in kcal/mol) for intermediates, transition states and products along the mechanistic pathway for the alkaline hydrolysis of acetanilide with participation of an explicit water molecule from HF/6-31+G(d) and B3LYP/6-31+G(d,p) calculations

	HF/6-31+G(d)		B3LYP/6-31+G(d,p)	
Structure	ΔE[a]	ΔG	ΔE[a]	ΔG
R[b]	0.00	0.00	0.00	0.00
C1–W-AA	−32.74	−22.96	—	—
TS1–W-AA	−6.12	6.48	−7.66	4.29
ITD*syn1*–W-AA[c]	−16.00	−5.19	−12.42	−1.55
ITD*syn2*–W-AA[c]	−18.11	−5.80	−14.35	−2.14
TS2*syn*–W-AA[c]	−9.56	3.43	−9.29	3.28
ITD*anti*–W-AA[c]	−3.85	8.40	−1.72	9.62
TS2*anti*–W-AA[c]	−1.38	11.18	9.92	22.21
P	−27.58	−35.50	−14.05	−23.65

[a] Corrected for zero-point vibrational energy.
[b] Reactants are the amide and the $[OH\ldots H_2O]^-$ complex.
[c] The different conformers of the intermediates and TS2 are illustrated in Fig. 1 in the case of **MBA**.

molecule makes a bridge between the two oxygen atoms, thus forming two relatively strong hydrogen bonds.

IRC computations from **TS1** lead to the subsequent minima in the reaction path. These are the tetrahedral intermediates interacting with the water molecule by forming $O^- \cdots HOH$ hydrogen bond. As a consequence the energies of these structures in the three amides also decrease. These results indicate that the explicit water molecule does not play a substantial catalytic role during the first stage of the hydrolysis process, though it stabilizes all structures through hydrogen bonding. The computed intrinsic free energy barriers for the water-assisted alkaline hydrolysis of **MBA**, **MAA**, and **AA** are compared in Table 7. The intrinsic energy barriers for the first step of the water-assisted hydrolysis, the addition process, as obtained from Hartree–Fock computations are 33.64 kcal/mol for **MBA**, 32.49 kcal/mol for **MAA**, and 29.44 kcal/mol for **AA**. The respective values for the non-assisted gas phase hydrolysis are 26.73, 25.45, and 26.28 kcal/mol. These values are estimated from the data presented in Tables 1–3. Therefore, the ancillary water molecule stabilizes all structures through hydrogen bond formation, while the intrinsic energy barrier heights for the first step of addition are distinctly higher than for the non-assisted gas-phase processes.

The elimination step of amide hydrolysis involves two main rearrangements: (a) a C—N bond cleavage, and (b) a hydrogen transfer from the acidic part toward the amine. The supporting role of the water molecule on the hydrogen transfer is well seen from the structures and transition vectors of **TS2*anti*** for assisted

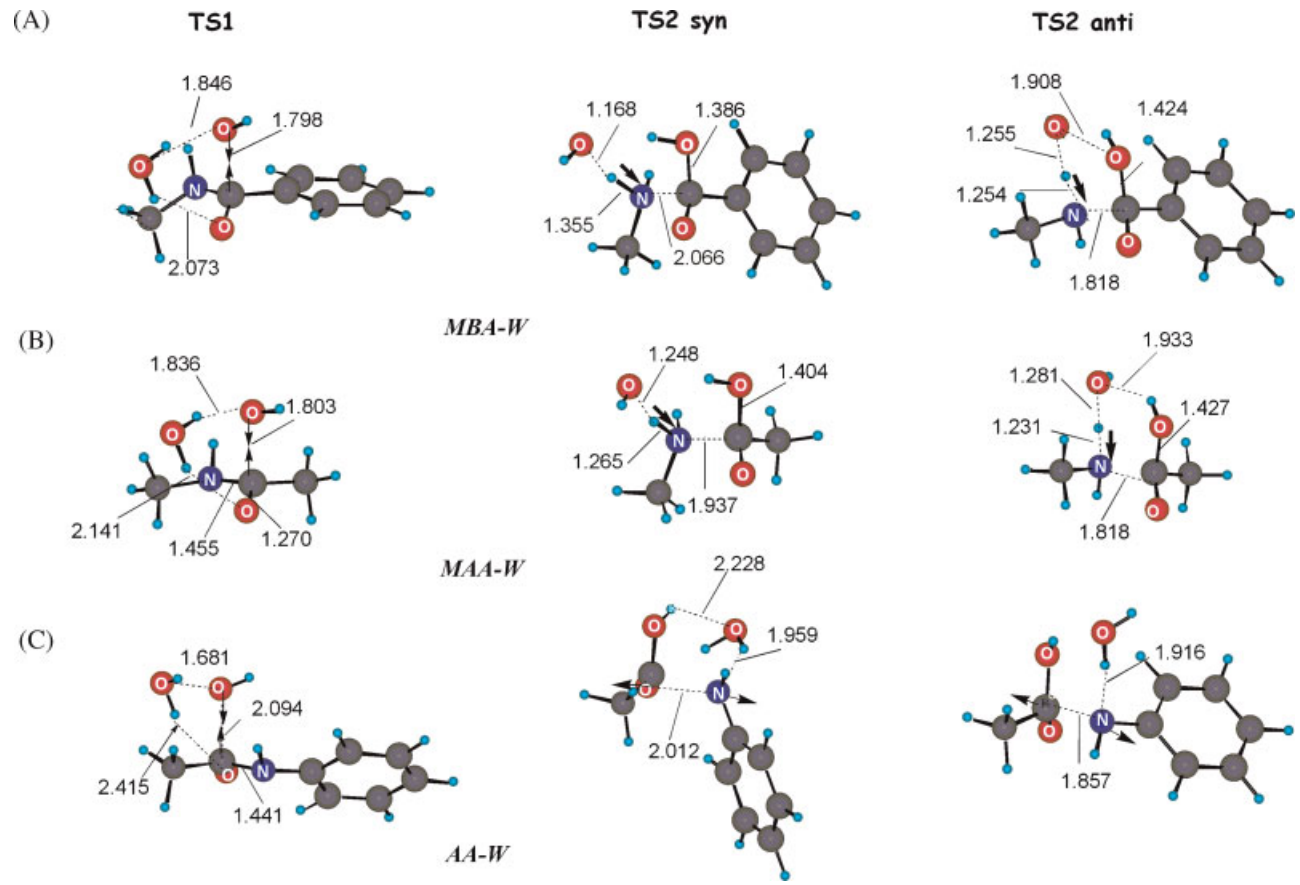

Figure 4. Transition state structures along the reaction pathways for water-assisted hydrolysis of MBA (A), MAA (B), and AA (C) from B3LYP/6-31+G(d,p) computations

Table 7. Computed intrinsic free energy barrier heights (at 1 atm, 298.15 K, in kcal/mol) for the water-assisted alkaline hydrolysis of *N*-methylbenzamide, *N*-mehtylacetamide, and acetanilide

Intrinsic activation barriers[a]	HF/6-31+G(d) $\Delta G^{\neq}$	B3LYP/6-31+G(d,p) $\Delta G^{\neq}$
MBA-W		
$\Delta G_1^{\neq}$	33.64	33.06
$\Delta G_{2syn}^{\neq}$	24.56	8.51
$\Delta G_{2anti}^{\neq}$	13.64	3.05
MAA-W		
$\Delta G_1^{\neq}$	32.49	33.27
$\Delta G_{2syn}^{\neq}$	24.04	10.14
$\Delta G_{2anti}^{\neq}$	12.5	3.90
AA-W		
$\Delta G_1^{\neq}$[b]	29.44	—
$\Delta G_{2syn}^{\neq}$	9.23	5.43
$\Delta G_{2anti}^{\neq}$[b]	2.79	2.29

[a] $\Delta G_1^{\neq} = G_{TS1} - G_{C1}$; $\Delta G_{2syn}^{\neq} = G_{TS2syn}$-$G_{ITDsyn}$; $\Delta G_{2anti}^{\neq} = \Delta G_{TS2anti} - \Delta G_{ITDanti}$.

[b] Single point DFT computations over HF/6-31+G(d) optimized structures.

MBA and **MAA** hydrolysis, presented in Fig. 4. It is seen that the transition vector corresponds mostly to a proton transfer. Thus the intrinsic free energy barrier for this step appears to be mostly determined from the proton transfer. The results obtained indicate that the ancillary water molecule facilitates the proton transfer processes for the hydrolysis of **MBA** and **MAA**.

As can be seen in Fig. 4C in the case of assisted hydrolysis of acetanilide (**AA**), the water molecule also stabilizes all the structure along the reaction path. The intrinsic free barrier heights determined for the second transition state are 9.23 and 2.79 kcal/mol for ***syn*** and ***anti*** conformers respectively (at HF level of computations). In contrast to the assisted hydrolysis for **MBA** and **MAA**, the principal component of the transition vector for the second transition state in the case of **AA** is the C—N bond cleavage. In both **TS2*syn*–W-AA** and **TS2*anti*–W-AA** structures the C—N bond is almost broken with a bond length of 2.086 and 1.857 Å respectively (at the HF level).

The computed intrinsic activation free energies for the second step of the water-assisted alkaline hydrolysis of **MBA**, **MAA**, and **AA** are presented in Table 7. A comparison of the energy profiles for the assisted hydrolysis of **MBA**, **MAA**, and **AA** is also illustrated in Fig. 5. The data show that the explicit water molecule lowers the intrinsic free energy barriers for the second step of hydrolysis by 6.47 kcal/mol in the case of **MBA** and by 2.19 kcal/mol for **MAA**. In the case of acetanilide, the leaving group is an aromatic amine anion. Because of the higher stability of $PhNH^-$, the proton transfer toward the leaving group, which stabilizes the anion, appears to be less important. Thus the ancillary water molecule does not influence significantly the free energy barrier associated with TS2 in the case of acetanilide. The results obtained indicate that in the case of **AA** the water molecule does not interfere into

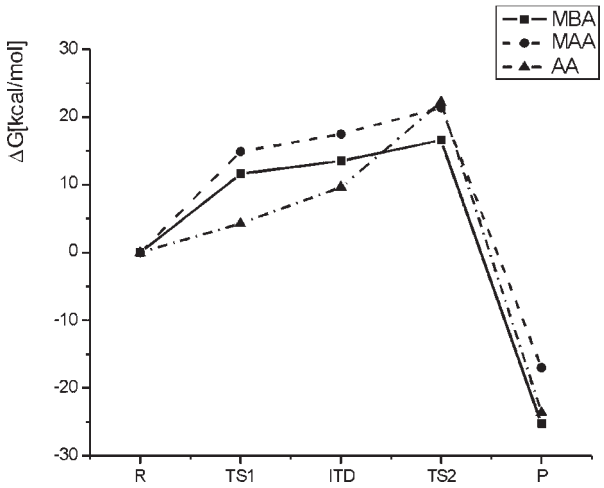

Figure 5. Energy profiles of water assisted hydrolysis of MBA, MAA, and AA from B3LYP/6-31+G(d,p) computations

the processes at the reaction center. When the leaving group is an aliphatic amine (in the cases of **MBA** and **MAA**) the proton transfer from the water molecule is essential for the stabilization of the $AlkNH^-$ anion. For these systems the ancillary water leads to substantially lower barrier for this reaction step. On the experimental side the role of the leaving group on the kinetics of basic hydrolysis in the case of substituted toluamides was discussed by Brown and co-workers.[26]

Table 8 shows the variation of Mulliken charges at the reaction centers going from initial reactants to **TS1**, **ITD**, and **TS2** for the water assisted process. It is seen that in **TS1**, **ITD**, **TS2** the net negative charges at the nitrogen and oxygen atoms of amide group are increased, while the net positive charge at the carbon

Table 8. Variations of Mulliken charges (in electrons) at the atoms of the water assisted alkaline hydrolysis of *N*-methylbenzamide, *N*-methylacetamide, and acetanilide from B3LYP/6-31+G(d,p) computations

Structures	q_C[a]	q_O[a]	q_N[a]	q_O[b]
MBA				
MBA	−0.0092	−0.5412	−0.3166	−1.0788
TS1	−0.1810	−0.5984	−0.4278	−0.7485
ITD	0.2632	−0.6851	−0.5698	−0.3981
TS2	0.2234	−0.5830	−0.6971	−0.3997
MAA				
MAA	0.4044	−0.5359	−0.3526	−1.0788
TS1	−0.0414	−0.6294	−0.3794	−0.7787
ITD	0.1722	−0.6690	−0.6378	−0.5132
TS2	0.2303	−0.6001	−0.7115	−0.4892
AA				
AA	0.7284	−0.5077	−0.3562	−1.0788
TS1	0.0879	−0.5544	−0.2919	−0.8622
ITD	0.3295	−0.5827	−0.4541	−0.4713
TS2	0.2157[c]	−0.5061[c]	−0.5903[c]	−0.4105[c]

[a] The atoms from the amide grouping.

[b] The oxygen atom originally from the $[OH...H_2O]^-$ complex.

[c] From the B3LYP/6-31+G(d,p)//HF/6-31+G(d) computations.

atom is substantially decreased. Thus a significant amount of the negative charge coming from the [OH^-...H_2O] complex is delocalized over the amide group. However, no emergence of zwitterionic structure throughout the reaction path is recorded. The zwitterionic structure involves a positive charge at the nitrogen atom. Such effect is not predicted by the theoretical computations carried out.

The combined effect of water as a reactive species and bulk solvent

In this subsection the role of water on the energy profiles of the alkaline hydrolysis of **MBA**, **MAA**, and **AA** is assessed by studying its role as a species assisting the various stages of the mechanism of the reactions as well as a bulk solvent. Such model treatment comes closer to the experimental processes. This approach has been successfully applied in theoretical treatments of ionic reactions in solution.[106,107] Xiong and Zhan[69] applied this procedure in their study on the alkaline hydrolysis of the base-catalyzed hydrolysis of the first transition state of formamide, *N*-methylacetamide, *N*,*N*-dimethylformamide and *N*,*N*-dimethylacetamide. These authors considered that the addition stage is the rate-limiting stage of the reaction.

All optimized structures of the stationary points along the pathways of the water-assisted hydrolysis of **MBA**, **MAA**, and **AA** were placed in a cavity of water solution and the relative to reactant Gibbs free energies were estimated by applying the IEFPCM SCRF method at the B3LYP/6-31+G(d,p) and MP2/6-31+G(d,p) levels of theory (Table 9). The results from both DFT and MP2 computations show that the overall process is exothermic for the three amides considered but with distinctive free energy barriers for the formation of the tetrahedral intermediates and their cleavage to products.

To verify further the reliability of the theoretical results obtained single point MP2 computations employing the 6-311++G(2d,2p) basis set combined with the IEFPCM method were carried out over geometries optimized at B3LYP/6-31+G(d,p) level of theory. The results obtained are presented in Table 10. The Gibbs free energies of the stationary points along the hydrolysis reaction paths for the three studied amides are illustrated in Fig. 6. The highest level of computations, MP2/6-311++G(2d,2p), reveals that the formation of the tetrahedral product in **AA** is associated with markedly lower free energy shift (23.75 kcal/mol) than in the cases of **MBA** (31.05 kcal/mol) and **MAA** (30.48 kcal/mol). The results (Table 10) show that for the **MAA** and **AA** the rate-determining stage of the alkaline hydrolysis is the formation of **TS2**. In the case of **MBA** the computations predict only slightly higher free energy of formation of the **TS2** compared to **TS1**.

Table 10. Relative to reactants Gibbs free energies, ΔG (at 1 atm, 298.15 K, in kcal/mol) for intermediates, transition states and products along the mechanistic pathway for the water assisted alkaline hydrolysis of **MBA**, **MAA**, and **AA**, in aqueous solution from MP2/6-311++G(2d,2p) IEFPCM computations[a]

Structures	MBA	MAA	AA
R[b]	0.00	0.00	0.00
TS1	31.05	30.48	23.75
ITD*syn*	21.03	23.76	18.11
TS2*syn*	36.49	36.99	28.05
ITD*anti*	24.94	26.97	23.40
TS2*anti*	31.25	33.08	28.69[c]
P	−13.13	−10.56	−16.63

[a] Single point computations over B3LYP/6-31+G(d,p) optimized geometry using UFF radii.
[b] Reactants are the amide and the [OH...H_2O]$^-$ complex.
[c] Single point computations over HF/6-31+G(d,p) optimized geometry.

Barrier heights from kinetic experiments

As already discussed, the free energy barrier heights for the alkaline hydrolysis of *N*-methylbenzamide and acetanilide were

Table 9. Relative to reactants Gibbs free energies, ΔG (at 1 atm, 298.15 K, in kcal/mol) for intermediates, transition states and products along the mechanistic pathway for the water assisted alkaline hydrolysis of **MBA**, **MAA**, and **AA**, in aqueous solution from IEFPCM computations at B3LYP/6-31+G(d,p) and MP2/6-31+G(d,p) level of theory

	MBA		MAA		AA	
Structure	I[a]	II[b]	I[a]	II[b]	I[a]	II[b]
R[c]	0.00	0.00	0.00	0.00	0.00	0.00
TS1	38.90	30.82	37.58	30.45	29.89	23.27
ITD*syn*	31.58	20.85	32.11	23.37	26.30	17.95
TS2*syn*	41.84	37.16	41.20	37.03	35.56	28.63
ITD*anti*	34.51	24.86	34.71	26.85	32.55	23.13
TS2*anti*	38.80	31.03	38.67	32.82	37.90[d]	30.21[d]
P	−14.49	−13.36	−11.55	−11.64	−19.25	−17.86

[a] IEFPCM B3LYP/6-31+G(d,p)//B3LYP/6-31+G(d,p) computations.
[b] IEFPCM MP2/6-31+G(d,p)// B3LYP/6-31+G(d,p) computations.
[c] Reactants are the amide and the [OH...H_2O]$^-$ complex.
[d] Single point computations over HF/6-31+G(d,p) optimized geometry.

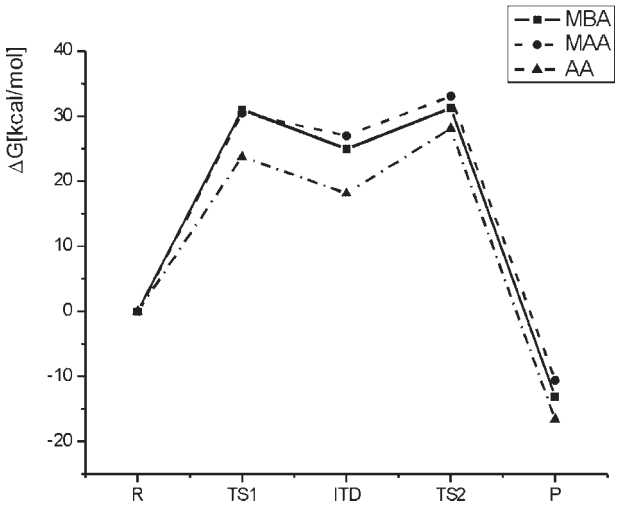

Figure 6. Energy profiles of water assisted hydrolysis of MBA, MAA, and AA from IEFPCM MP2/6-311++G(2d,2p) computations. The lowest energy TS2 structures are included

experimentally determined in the present study. The respective value for the reaction of *N*-methylacetamide was deduced from literature variable temperature kinetic data.[105] The experimental free energies of activation for the alkaline hydrolysis of **MBA**, **AA**, and **MAA** are given in Table 11. These values are compared with theoretically estimated barrier heights determined at MP2/6-311++G(2d,2p) level fo theory. The computational results shown reflect the combined effect of water as a reactive species and bulk solvent. It is seen that the theoretically predicted values are distinctly higher for all three molecules studied. Warshel and co-workers[61] have pointed out that the theoretical computations referring to gas phase processes overestimate considerably the entropy effects. To assess the possible errors coming from the entropy term we calculated separately the enthalpy and the entropy contributions to the free energies and compared them with the experimental values. The theoretically estimated $\Delta H^{\neq}$ and $\Delta S^{\neq}$ values for the reaction associated with the rate-determining stage of reaction coming from MP2/6-311++G(2d,2p) computations are presented in Table 11. These values are compared with the respective experimental quantities. A very good correspondence between theoretical and experimental $\Delta H^{\neq}$ values for the hydrolysis of all three molecules studied is obtained. It is clearly seen, however, that the theoretically estimated entropy term are seriously overestimated and are the principal reason for the disaccord between predicted and experimental free energy barriers. As already emphasized the entropy terms are evaluated for gas phase processes.

Table 11. Comparison of theoretically estimated from MP2/6-311++G(2d,2p) computations and experimental values for the Gibbs free energies (at 1 atm, 298.15 K, in kcal/mol), enthalpies of activation (kcal/mol), entropies of activation (in cal/(mol K)) for the alkaline hydrolysis of *N*-methylbenzamide, acetanilide, and *N*-methylacetamide[a,b]

$\Delta G^{\neq}$	$\Delta H^{\neq}$	$\Delta S^{\neq}$	$\Delta G^{\neq}_{exp}$ [e]	$\Delta H^{\neq}_{exp}$ [e]	$\Delta S^{\neq}_{exp}$ [e]
N-Methylabenzamide[c]					
31.25	17.13	−47.34	23.21	16.41	−22.81
Acetanilide[c]					
28.05	14.32	−46.04	22.15	12.18	−33.41
N-Methylacetamide[d]					
33.08	18.00	−50.57	22.94	17.06	−19.73

[a] The theoretical results include consideration of explicit water molecule and IEFPCM level of theory computations (UFF radii) of the bulk water solvent effect.
[b] For details of computations see footnotes to Tables 8 and 9.
[c] This work.
[d] Calculated using the kinetic data from Ref [105].
[e] Calculated using the Eyring equation.

Relative reactivities

The relative reactivities for the base hydrolysis of the studied amides can be rationalized considering the intramolecular electronic effects influencing the electronic structure of the reaction center. Theoretically evaluated quantities characterizing the charge densities in the studied molecules are presented in Table 12. These are the NBO charges[108–110] ($q_{X(C=O)}$) at the carbon and oxygen atoms of the carbonyl bond as well as the electrostatic potential values[111,112] at the carbonyl carbon ($V_{C(C=O)}$). These quantities were obtained for aqueous solution of the reactant amides using the IEFPCM method on fully optimized B3LYP/6-31+G(d,p) structures. The conjugative effects in the two types of aromatic amides can be assessed by comparisons with the respective data for *N*-methylacetamide. The partial positive charge at the reaction center, the carbonyl carbon, is determined by the differing electronegativity of the two atoms forming the carbonyl bond. Another factor is the resonance and inductive interactions between C═O and the nitrogen atom.

The predominant resonance effect of the nitrogen lone pair is expected to result in increased negative charge at the carbonyl oxygen. The hyperconjugation with the adjacent methyl group further adds to this influence. The negative inductive effect of the nitrogen, on the other hand, attracts electron density from the neighboring carbonyl carbon. In **MBA** the conjugation between C═O and the aromatic ring results in partial transfer of a negative charge from the oxygen toward the ring. The computations (Table 12) show that the negative charge at the oxygen is reduced, in accord with expectations. The positive charge at the carbonyl carbon is also lowered by such substitution. It may, therefore, be concluded that the addition process will be less favored in **MBA** than in **MAA**. The theoretically estimated $\Delta H^{\neq}$ values for these molecules (Table 11) are in accord with these charge effects. In the case

Table 12. NBO atomic charges (q^{NBO}, in electrons) and electrostatic potentials (V_X, in a.u.) at the atoms of the reaction center from IEFPCM B3LYP/6-31+G(d,p) computations

Compound	$q^{NBO}_{C(C=O)}$	$q^{NBO}_{O(C=O)}$	$V_{C(C=O)}$
MBA	0.6795	−0.7056	−14.6398
MAA	0.6847	−0.7286	−14.6360
AA	0.6970	−0.6928	−14.6210

of **AA**, the nitrogen lone pair is engaged in competitive conjugation with both C═O and the adjacent aromatic ring. Thus, the transfer of negative charge from the nitrogen toward C═O is reduced. The partial positive charge at the carbonyl carbon becomes higher and facilitates the attack by the nucleophile. Another useful quantity, which has been shown to predict well reactivity[78,113–119] is the electrostatic potential at the atoms (V_X) of the reaction center in the reactants. The computed ($V_{C(C=O)}$) values in **MBA** and **MAA** are quite close. This result is in accord with the very similar energetics of the reactions in **MBA** and **MAA** (Table 9). Less negative electrostatic potential in the case of **AA** clearly illustrates the reduced electron density of the reaction center, which favors the attack by the hydroxide ion.

The above considerations refer to the relative reactivities of the three amides with respect the addition stage of the reaction, which is directly influenced by the electronic structure of the reactants. The charge densities in the reactants, therefore, may only qualitatively be used in discussing the overall reactivities of the molecules in the alkaline hydrolysis process. As we have seen from the data illustrated in Figs 3, 5, and 6, the heights of the energy barriers for the rate-determining stage of the process depend strongly on the structure of the leaving group.

The overall reactivity in this series of compounds is, in general, governed not only by the enthalpy related effects but also by entropy variations. As we have seen, however, the predictions of the $\Delta S^{\neq}$ terms, coming from theoretical computations for the reactions in gas phase, are drastically overestimated (Table 11).

The results indicate that the overall reactivity of the secondary amides in the base hydrolysis reaction would depend on the balance between several principal factors: (a) the electron attracting ability of the carbonyl carbon of the reactants; (b) the stability of the leaving group; (c) the solvating effects of the aqueous solvent, which can influence selectively the barrier height for the rate-determining stage of the process for different secondary amides.

CONCLUSIONS

A comprehensive computational study of the alkaline hydrolysis for three secondary amides is carried: *N*-methylbenzamide, *N*-methylacetamide, and acetanilide. The role of water on the reaction mechanism and energy profile is examined. The theoretical results are supplemented by experimental determination of the barrier heights for the hydrolysis of *N*-methylbenzamide and acetanilide. The results obtained show that:

- In the cases of *N*-methylbenzamide and *N*-methylacetamide the process is catalyzed by an ancillary water molecule, which facilitates the proton transfer processes. In the case of acetanilide the ancillary water molecule is found to stabilize the critical points along the reaction path just by solvation.
- The alkaline hydrolysis assisted by the ancillary water molecule in aqueous solvent is characterized by two distinct free energy barriers associated with the formation of a tetrahedral adduct by the reactants and its breaking to products.
- The reaction is exothermic for all three studied amides.
- The results show that for the studied amides the rate-determining stage of the reaction is associated with the second transition state: the cleavage of the tetrahedral adduct to product. In the case of **MBA**, the free energy barrier for the second transition state is only slightly higher than the barrier heights for the first transition state.
- The overall reactivity of the secondary amides in the base hydrolysis reaction is governed by the balance between several principal factors: (a) the electron attracting ability of the carbonyl carbon of the reactants; (b) the stability of the leaving group; (c) the solvating effects of the aqueous solvent, which can influence selectively the barrier height of the rate-determining stage of the process for different secondary amides.
- A good correspondence between experimentally determined enthalpies of activation of the processes and theoretical predictions coming from MP2/6-311++G(2d,2p) computations is obtained.
- The entropy contributions to free energy barriers obtained from B3LYP/6-31+G(d,p) computations referring to gas-phase processes are strongly overestimated compared to experiment.

SUPPORTING INFORMATION

Cartesian coordinates, electronic energies in Hartree and the number of imaginary frequencies for B3LYP/6-31+G(d,p) fully optimized geometries of all the structures along the reaction path for the alkaline hydrolysis of *N*-methylbenzamide in gas phase and for water-assisted mechanism of the three amides studied. Details of the kinetic results are also provided.

Acknowledgements

This research was supported by the National Science Fund (Bulgaria), Grant VU-X04/05.

REFERENCES

[1] R. S. Brown, in *The Amide Linkage: Selected Structural Aspects in Chemistry, Biochemistry, and Materials Science* (Ed.: C. M. Breneman, A. Greenberg, J. F. Liebman), Wiley Interscience, New York, **1999**. p. 85.
[2] M. L. Bender, *Chem. Rev.* **1960**, *60*, 53.
[3] M. L. Bender, R. D. Ginger, K. C. Kemp, *J. Am. Chem. Soc.* **1954**, *76*, 3350.
[4] P. M. Mader, *J. Am. Chem. Soc.* **1965**, *87*, 3191.
[5] M. L. Bender, R. J. Thomas, *J. Am. Chem. Soc.* **1961**, *8*, 4183.
[6] S. S. Biechler, R. W. Taft, *J. Am. Chem. Soc.* **1957**, *79*, 4927.
[7] M. L. Bender, R. D. Ginger, J. P. Unik, *J. Am. Chem. Soc.* **1958**, *80*, 1044.
[8] C. A. Bunton, D. N. Spatcher, *J. Chem. Soc.* **1956**, 1079.
[9] R. L. Schowen, G. W. Zuorick, *J. Am. Chem. Soc.* **1966**, *88*, 1223.
[10] R. L. Schowen, H. Jayaraman, L. Kershner, *J. Am. Chem. Soc.* **1966**, *88*, 3373.
[11] R. L. Schowen, H. Jayaraman, L. Kershner, G. W. Zuorick, *J. Am. Chem. Soc.* **1966**, *88*, 4008.
[12] L. D. Kershner, R. L. Schowen, *J. Am. Chem. Soc.* **1971**, *93*, **2014**.
[13] I. H. Williams, G. M. Maggiora, R. L. Schowen, *J. Am. Chem. Soc.* **1980**, *102*, 7831.
[14] J. K. Young, S. Pazhanisamy, R. L. Schowen, *J. Org. Chem.* **1984**, *49*, 4148.
[15] S. O. Eriksson, *Acta Chem. Scand.* **1966**, *20*, 1892.
[16] S. O. Eriksson, *Acta Chem. Scand.* **1968**, *22*, 892.
[17] S. O. Eriksson, *Acta Pharm. Suecica.* **1969**, *6*, 139.
[18] R. M. Polack, M. L. Bender, *J. Am. Chem. Soc.* **1970**, *92*, 7190.
[19] R. M. Polack, T. C. Dumsha, *J. Am. Chem. Soc.* **1973**, *95*, 4463.
[20] R. H. DeWolfe, R. C. Newcomb, *J. Org. Chem.* **1971**, *25*, 3870.
[21] J. P. Guthrie, *J. Am. Chem. Soc.* **1974**, *96*, 3608.

[22] K. Bowden, K. Bromley, *J. Chem. Soc. Perkin Trans.* **1990**, *2*, 2103.
[23] H. Slebocka-Tilk, A. J. Bennet, H. J. Hogg, R. S. Brown, *J. Am. Chem. Soc.* **1991**, *113*, 1288.
[24] H. Slebocka-Tilk, F. Sauriol, M. Monette, R. S. Brown, *Can. J. Chem.* **2002**, *80*, 1343.
[25] H. Slebocka-Tilk, A. Neverov, R. S. Brown, *J. Am. Chem. Soc.* **2003**, *125*, 1851.
[26] H. Slebocka-Tilk, A. J. Bennet, J. W. Keillor, J. P. Brown, R. S. Gutrie, A. Jodhan, *J. Am. Chem. Soc.* **1990**, *112*, 8507.
[27] R. S. Brown, A. J. Bennet, H. Slebocka-Tilk, *Acc. Chem. Res.* **1992**, *25*, 481.
[28] J. F. Marlier, *J. Am. Chem. Soc.* **1993**, *115*, 5953.
[29] J. F. Marlier, N. C. Dopke, K. R. Johnstone, T. J. Wirdzig, *J. Am. Chem. Soc.* **1999**, *121*, 4356.
[30] P. D. Bolton, *Aust. J. Chem.* **1966**, *19*, 1013.
[31] P. D. Bolton, G. L. Jackson, *Aust. J. Chem.* **1971**, *24*, 969.
[32] V. Gani, P. Viout, *Tetrahedron* **1976**, *32*, 1669.
[33] C. A. Bunton, B. Nayak, C. O'Connor, *J. Org. Chem.* **1968**, *33*, 572.
[34] T. Sotomasu, T. Fujita, *J. Org. Chem.* **1989**, *54*, 4443.
[35] R. A. Cox, K. Yates, *Can. J. Chem.* **1981**, *59*, 1391.
[36] I. Meloche, K. J. Laidler, *J Am. Chem. Soc.* **1951**, *73*, 1712.
[37] U. Meresaar, L. Bratt, *Acta Chem. Scand. A* **1974**, *28*, 751.
[38] G. M. Blackburn, D. J. Plackett, *J. Chem. Soc. Perkin Trans. 2*, **1972**, 1366.
[39] G. M. Blackburn, C. J. Skaife, I. T. Kay, *J. Chem. Res.* **1988**, 294.
[40] N. J. Buurma, M. J. Blandamer, J. B. F. N. Engberts, *J. Phys. Org. Chem.* **2003**, *16*, 438.
[41] T. H. Fife, R. Bembi, *J. Am. Chem. Soc.* **1993**, *115*, 11358.
[42] W. J. Tenn III, N. L. French, R. W. Nagorski, *Org. Lett.* **2003**, *3*, 75.
[43] R. M. Smith, D. E. Hansen, *J. Am. Chem. Soc.* **1998**, *120*, 8910.
[44] H. B. Burgi, J. D. Dunitz, J. M. Lehn, G. Wipff, *Tetrahedron* **1974**, *30*, 1563.
[45] G. Alagona, E. Scrocco, J. Tomasi, *J. Am. Chem. Soc.* **1975**, *97*, 6976.
[46] S. Scheiner, W. N. Lipscomb, D. A. Kleier, *J. Am. Chem. Soc.* **1976**, *98*, 4770.
[47] G. M. Maggiora, I. H. Williams, *J. Mol. Struct. (Theochem.)* **1982**, *88*, 23.
[48] J. D. Madura, W. L. Jorgensen, *J. Am. Chem. Soc.* **1986**, *108*, 2517.
[49] O. N. Ventura, E. L. Coitino, A. Lledos, J. Bertran, *J. Comp. Chem.* **1992**, *13*, 1037.
[50] K. Hori, A. Kamimura, K. Ando, M. Mizumura, Y. Ihara, *Tetrahedron* **1988**, *53*, 4317.
[51] K. Hori, Y. Hashitani, Y. Kaku, K. Ohkubo, *J. Mol. Struct. (Theochem.)* **1999**, *461–462*, 589.
[52] J. P. Krug, P. L. A. Popelier, R. F. W. Bader, *J. Phys. Chem.* **1992**, *96*, 7604.
[53] J. S. Francisco, I. H. Williams, *J. Am. Chem. Soc.* **1993**, *115*, 3746.
[54] S. Antonczak, M. F. Ruiz-Lopez, J. L. Rivail, *J. Am. Chem. Soc.* **1994**, *116*, 3912.
[55] S. Antonczak, M. F. Ruiz-Lopez, J. L. Rivail, *J. Mol. Model.* **1997**, *3*, 434.
[56] S. Antonczak, G. Monard, M. F. Ruiz-Lopez, J. L. Rivail, *J. Am. Chem. Soc.* **1998**, *120*, 8825.
[57] S. J. Weiner, U. C. Singh, P. A. Kollman, *J. Am. Chem. Soc.* **1985**, *107*, 2219.
[58] A. E. Howard, P. A. Kollman, *J. Am. Chem. Soc.* **1988**, *110*, 7195.
[59] D. Bakowies, P. A. Kollman, *J. Am. Chem. Soc.* **1999**, *121*, 5712.
[60] S. Chalmet, W. Harb, M. F. Ruiz-López, *J. Phys. Chem. A.* **2001**, *105*, 11574.
[61] M. Strajbl, J. Florian, A. Warshel, *J. Am. Chem. Soc.* **2000**, *122*, 5354.
[62] D. Zahn, *Chem. Phys. Lett.* **2004**, *383*, 134.
[63] D. Zahn, *Chem. Phys.* **2004**, *300*, 79.
[64] D. Zahn, *J. Phys. Chem. B* **2003**, *107*, 12303.
[65] D. Zahn, *Eur. J. Org. Chem.* **2004**, *10*, 4020.
[66] V. A. Basiuk, H. M. Montiel, *Adv. Space Res.* **2005**, *36*, 209.
[67] J. F. O'Brien, J. Pranata, *J. Phys. Chem.* **1995**, *99*, 12759.
[68] Y. J. Zheng, R. L. Ornstein, *J. Mol. Struct. (Theochem.)* **1998**, *41*, 429.
[69] Y. Xiong, C. Zhan, *J. Phys. Chem. A* **2006**, *110*, 12644.
[70] J. Pitarch, M. F. Ruiz-Lopez, J. L. Pascual-Ahuir, E. Silla, I. Tunon, *J. Phys. Chem. B* **1997**, *101*, 3581.
[71] J. Pitarch, M. F. Ruiz-Lopez, E. Silla, J. L. Pascual-Ahuir, I. Tunon, *J. Am. Chem. Soc.* **1998**, *120*, 2146.
[72] J. Pitarch, J. L. Pascual-Ahuir, E. Silla, I. Tunon, V. Moliner, *J. Chem. Soc. Perkin Trans. 2*, **1999**, 1351.
[73] J. Pitarch, J. L. Pascual-Ahuir, E. Silla, I. Tunon, M. F. Ruiz-Lopez, C. Millot, J. Bertran, *Theor. Chem. Acc.* **1999**, *101*, 336.
[74] L. Gorb, A. Asensio, I. Tuñón, M. F. Ruiz-López, *Chem Eur. J.* **2005**, *11*, 6743.
[75] X. Lopez, J. I. Mujika, G. M. Blackburn, M. Karplus, *J. Phys. Chem. A* **2003**, *107*, 2304.
[76] J. I. Mujika, J. M. Mercero, X. Lopez, *J. Am. Chem. Soc.* **2005**, *127*, 4445.
[77] D. Cheshmedzhieva, S. Ilieva, B. Galabov, *J. Mol. Struct. (Theochem.)* **2004**, *681*, 105.
[78] B. Galabov, D. Cheshmedzhieva, S. Ilieva, B. Hadjieva, *J. Phys. Chem. A* **2004**, *108*, 11457.
[79] J. R. Pliego Jr., J. M. Riveros, *Chem Eur. J.* **2002**, *8*, **1945**.
[80] J. R. Pliego Jr., *Chem. Phys.* **2004**, *306*, 273.
[81] J. Blumberger, M. Klein, *Chem. Phys. Lett.* **2006**, *422*, 210.
[82] B. Kallies, R. Mitzner, *J. Mol. Model.* **1998**, *4*, 183.
[83] M. Cascella, S. Raugei, P. Carloni, *J. Phys. Chem. B* **2004**, *108*, 369.
[84] V. Pelmenschnikov, M. R. A. Blomberg, P. E. M. Siegbahn, *J. Biol. Inorg. Chem.* **2002**, *7*, 284.
[85] G. A. Petersson, T. G. Tensfeldt, J. A. Montgomery Jr., *J. Chem. Phys.* **1991**, *94*, 6091.
[86] A. D. Becke, *J. Chem. Phys.* **1993**, *98*, 5648.
[87] C. W. Lee, R. G. Yang Parr, *Phys. Rev. B* **1988**, *37*, 785.
[88] T. Clark, J. Chandrasekhar, G. W. Spitznagel, P. V. R. Schleyer, *J. Comp. Chem.* **1983**, *4*, 294.
[89] C. Peng, P. Y. Ayala, H. B. Schlegel, M. J. Frisch, *J. Comp. Chem.* **1996**, *17*, 49.
[90] W. J. Hehre, L. Radom, P. V. R. Schleyer, J. Pople, in *Ab Initio Molecular Orbital Theory*, Wiley Interscience, New York, **1986**. p. 63.
[91] C. Gonzalez, H. B. Schlegel, *J. Chem. Phys.* **1989**, *90*, 2154.
[92] M. J. Frisch, G. W. Trucks, H. B. Schlegel, G. E. Scuseria, M. A. Robb, J. R. Cheeseman, V. G. Zakrzewski, J. A. Montgomery,, Jr., R. E. Stratmann, J. C. Burant, S. Dapprich, J. M. Millam, A. D. Daniels, K. N. Kudin, M. C. Strain, O. Farkas, J. Tomasi, V. Barone, M. Cossi, R. Cammi, B. Mennucci, C. Pomelli, C. Adamo, S. Clifford, J. Ochterski, G. A. Petersson, P. Y. Ayala, Q. Cui, K. Morokuma, D. K. Malick, A. D. Rabuck, K. Raghavachari, J. B. Foresman, J. Cioslowski, J. V. Ortiz, A. G. Baboul, B. B. Stefanov, G. Liu, A. Liashenko, P. Piskorz, I. Komaromi, R. Gomperts, R. L. Martin, D. J. Fox, T. Keith, M. A. Al-Laham, C. Y. Peng, A. Nanayakkara, C. Gonzalez, M. Challacombe, P. M. W. Gill, B. Johnson, W. Chen, M. W. Wong, J. L. Andres, C. Gonzalez, M. Head-Gordon, E. S. Replogle, J. A. Pople, *Gaussian 98 (Revision A.7); Gaussian, Inc.: Pittsburgh, PA*, **1998**.
[93] E. Cances, B. Mennucci, J. Tomasi, *J. Chem. Phys.* **1997**, *107*, 3032.
[94] J. Tomasi, M. Persico, *Chem. Rev.* **1994**, *94*, **2027**.
[95] M. J. Frisch, G. W. Trucks, H. B. Schlegel, G. E. Scuseria, M. A. Robb, J. R. Cheeseman, J. A. Montgomery Jr., T. Vreven, K. N. Kudin, J. C. Burant, J. M. Millam, S. S. Iyengar, J. Tomasi, V. Barone, B. Mennucci, M. Cossi, G. Scalmani, N. Rega, G. A. Petersson, H. Nakatsuji, M. Hada, M. Ehara, K. Toyota, R. Fukuda, J. Hasegawa, M. Ishida, T. Nakajima, Y. Honda, O. Kitao, H. Nakai, M. Klene, X. Li, J. E. Knox, H. P. Hratchian, J. B. Cross, C. Adamo, J. Jaramillo, R. Gomperts, R. E. Stratmann, O. Yazyev, A. J. Austin, R. Cammi, C. Pomelli, J. W. Ochterski, P. Y. Ayala, K. Morokuma, G. A. Voth, P. Salvador, J. J. Dannenberg, V. G. Zakrzewski, S. Dapprich, A. D. Daniels, M. C. Strain, O. Farkas, D. K. Malick, A. D. Rabuck, K. Raghavachari, J. B. Foresman, J. V. Ortiz, Q. Cui, A. G. Baboul, S. Clifford, J. Cioslowski, B. B. Stefanov, G. Liu, A. Liashenko, P. Piskorz, I. Komaromi, R. L. Martin, D. J. Fox, T. Keith, M. A. Al-Laham, C. Y. Peng, A. Nanayakkara, M. Challacombe, P. M. W. Gill, B. Johnson, W. Chen, M. W. Wong, C. Gonzalez, J. A. Pople, *Gaussian 03 (Revision A.1), Gaussian Inc., Pittsburgh PA*, **2003**.
[96] A. K. Rappe, C. J. Casewit, K. S. Colwell, W. A. Goddard,, III, W. M. Skiff, *J. Am. Chem. Soc.* **1992**, *114*, 10024.
[97] C. Moller, M. S. Plesset, *Phys. Rev.* **1934**, *46*, 618.
[98] J. A. Pople, J. S. Binkley, R. Seeger, *Int. J. Quantum Chem. Symp.* **1976**, *10*, 1.
[99] R. Krishnan, J. A. Pople, *Int. J. Quantum Chem.* **1978**, *14*, 91.
[100] R. Krishnan, M. J. Frisch, J. A. Pople, *J. Chem. Phys.* **1980**, *72*, 4244.
[101] K. Raghavachari, J. A. Pople, E. S. Replogle, M. Head-Gordon, *J. Phys. Chem.* **1990**, *94*, 5579.
[102] R. Krishnan, J. S. Binkley, R. Seeger, J. A. Pople, *J. Chem. Phys.* **1980**, *72*, 650.
[103] K. Vierordt, *Die Anwendung d. Spektralapparates zur Photometrie der Absorptionsspektren und zur quantitativen chemischen Analyse, Teubingen*, **1873**, p. 28.
[104] V. Pelmenschnikov, P. E. M. Siegbahn, *Inorg. Chem.* **2002**, *41*, 5659.

[105] Y. V. Moiseev, E. Y. Bakhrakh, M. I. Vinnik, *Zh. Fiz. Khim. (Russ.)* **1963**, *37*, 784.
[106] J. R. Pliego Jr., J. M. Riveros, *J. Phys. Chem. A* **2001**, *105*, 7241.
[107] J. R. Pliego Jr., J. M. Riveros, *J. Phys. Chem. A* **2002**, *106*, 7434.
[108] A. E. Reed, L. A. Curtiss, F. Weinhold, *Chem. Rev.* **1988**, *88*, 899.
[109] J. E. Carpenter, F. Weinhold, *J. Mol. Struct. (Theochem.)* **1988**, *169*, 41.
[110] E. D. Glendening, A. E. Reed, J. E. Carpenter, F. Weinhold, *NBO Version 3.1*.
[111] E. B. Wilson Jr., *J. Chem. Phys.* **1962**, *36*, 2232.
[112] P. Politzer, in *Chemical Applications of Atomic and Molecular Electrostatic Potentials* (Eds.: P. Politzer, D. G. Truhlar), Plenum Press, New York. **1981**, p. 7.
[113] P. Bobadova-Parvanova, B. Galabov, *J. Phys. Chem. A* **1998**, *102*, 1815.
[114] B. Galabov, P. Bobadova-Parvanova, *J. Phys. Chem. A* **1999**, *103*, 6793.
[115] V. Dimitrova, S. Ilieva, B. Galabov, *J. Phys. Chem. A* **2002**, *106*, 11801.
[116] B. Galabov, P. Bobadova-Parvanova, S. Ilieva, V. Dimitrova, *J. Mol. Struct. (Theochem.)* **2003**, *630*, 101.
[117] B. Galabov, S. Ilieva, H. F. Schaefer, *J. Org. Chem.* **2006**, *71*, 6382.
[118] B. Galabov, S. Ilieva, B. Hadjieva, Y. Atanassov, H. F. Schaefer, *J. Phys. Chem. A* **2008**, *112*, 6700.
[119] B. Galabov, V. Nikolova, J. J. Wilke, H. F. Schaefer, W. D. Allen, *J. Am. Chem. Soc.* **2008**, *130*, 9887.

